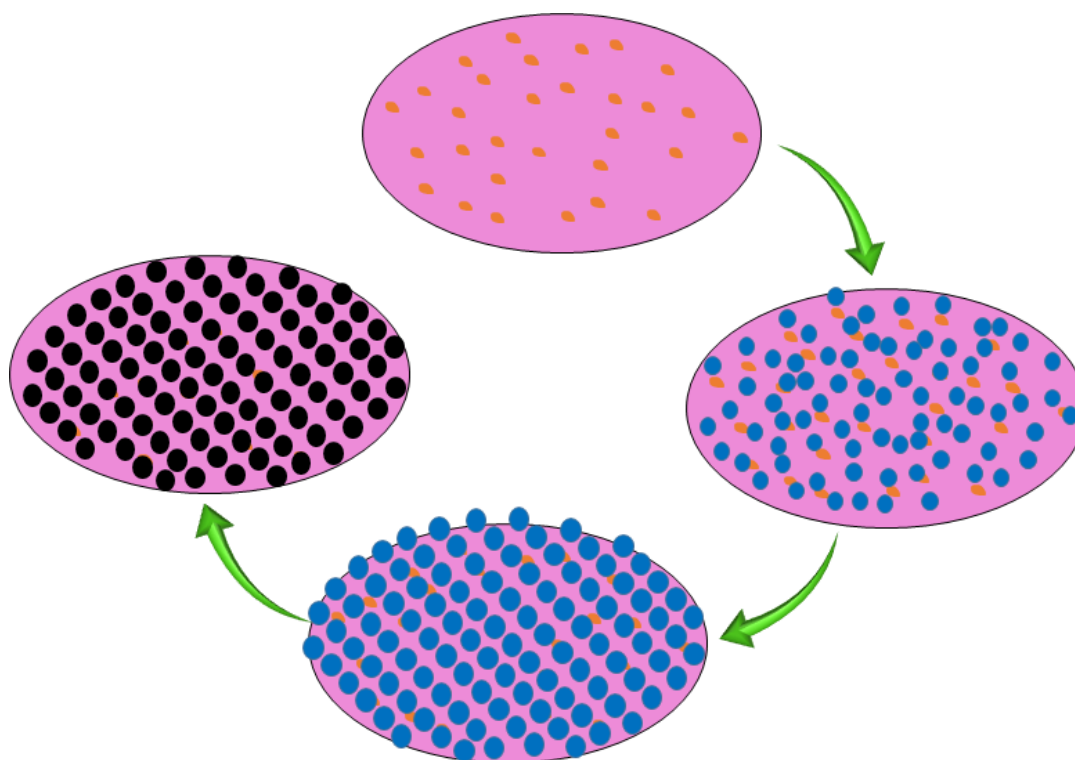

**MICROPATTERNED POLYSTYRENE-ALUMINA HYBRID
FILMS WITH AMINO-FUNCTIONALIZED BREATH-FIGURE
CAVITIES FROM THF**



3.1. ABSTRACT

Micropatterned polystyrene-alumina hybrid films with amino-functionalized breath figure (BF) cavities were fabricated with the aid of amino-functionalized amphiphilic alumina (SA) nanoparticles. Breath figures were produced by drying off the drop cast of SA particle suspension in polystyrene/THF solution (PSA suspensions) under ambient conditions. The concentration dependent morphological variation of BF pattern was studied by varying the suspension concentration. The influences of various factors such as particle concentration, hydrophobic/hydrophilic balance of the particle and silane-modifier ratio etc. on the

microstructure were studied. Formation of amino-functionalized cavities has been proven by the fluorescence microscopic images of fluorescamine treated hybrid film. Particle-assisted BF formation has been established.

3.2. INTRODUCTION

Conventionally, breath figure patterned films with functionalised cavities have been obtained by *in-situ* approach (Nishida *et al.*, 2002; Nyström *et al.*, 2010), employing polymers with polar functional groups, polymers containing functionalised oligomeric species etc., and by *ex-situ* approach (Samanta *et al.*, 2011) involving post-modification of the un-functionalised cavities. While the *in-situ* approach yielded functionality enriched cavities along with functionality present on the entire surfaces of the film, the *ex-situ* approach was tedious due to the involvement of various chemical processes. Particle-assisted breath figure formation provides a convenient method for producing functionalised cavities by *in-situ* approach (Boker *et al.*, 2004 ; Nair *et al.*, 2010). During the formation of BF cavities, the functionalised particles preferably migrate to the BF interface to functionalise the cavities. They were generally prepared by 'dispersing' or '*in-situ*' generation of inorganic nanoparticles in the polymer solution. Whereas *in-situ* generation is limited to nano metal particles and associated properties, dispersion method provides wide possibilities of using functionalised nano particles having wide range of functionality.

There have been several efforts to utilize functionalized nanoparticles as BF components to achieve particle-functionalized BF cavities in polymer hybrid films. These particles were either hydrophobic-modified (Boker *et al.*, 2004) or hydrophilic in nature (Sun *et al.*, 2008; Sun *et al.*, 2010). However, they posed certain disadvantages. The hydrophobic particles reside in the polymer phase inside the

cavity walls therefore the desired functionality is not exposed for applications. On the other hand, the hydrophilic particles were observed at the pore walls (figure 3.1) which make them vulnerable to various external forces during applications. Moreover, the particles had to be dispersed in ethanol, which acted as a 'solvent-surfactant', for dispersion of the hydrophilic particles in hydrophobic organic solvents used for preparing the BF patterns (Sun *et al.*, 2008; Sun *et al.*, 2010; Wan *et al.*, 2012). The microstructure of BF patterns was dependant on the concentration of alcohol in the suspension. On the other hand, amphiphilic particles disperse in wide range of solvents without the aid of alcohol. Moreover, they are likely to reside inside the cavity walls exposing the hydrophilic functional group at the surfaces, making them resistant to external forces.

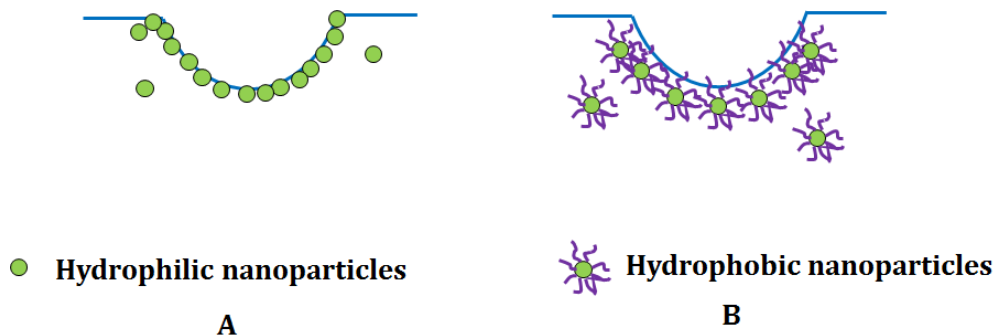


Figure 3.1. Schematic of functionalized BF cavities by (A) hydrophilic and (B) hydrophobic nanoparticles

Drop cast method has been widely used for the preparation of breath figures in polymer films because of its simplicity, ease of production and does not require any sophisticated fabrication techniques. In this chapter, utilization of amino-functionalised amphiphilic alumina nanoparticles (see chapter 1) for the preparation of BF patterned polystyrene films with amino-functionalised cavities is described.

Polystyrene was BF incompatible and THF was used as solvent for preparing the solution/suspension. The effects of variable factors like particle concentration, hydrophobic/ hydrophilic balance of the particle and silane-modifier ratio on microstructure and morphology of BF cavities are reported.

3.3. EXPERIMENTAL

3.3.1. Materials:

The materials used were Alumina powder (aps. 100nm, Sumitomo Corporation, Japan), Polystyrene (GPPS, local source), 3-aminopropyltriethoxysilane (AS), vinyltriethoxysilane (VS), Styrene (Aldrich Chemicals), Benzoyl peroxide (S.D Fine Chemicals Ltd, India), Tetrahydrofuran (THF) (Synthetic reagents, Merck Specialties Pvt. Ltd., India).

3.3.2. Fabrication of breath figure patterned polystyrene- alumina hybrid films

Suspensions of alumina particles in polystyrene solution (PSA suspensions) were used for the fabrication of micropatterned hybrid films. The suspensions were prepared by dispersing the amphiphilic-alumina (SA) particles, in polystyrene/THF solution. The amount of the particles was varied from 0 to 5 wt % of polystyrene. PSA suspension was ultrasonically mixed and drop cast (3 μ L) on a glass slide within 2 minutes. It was then dried at ambient temperature of \sim 30 $^{\circ}$ C and humidity of \sim 70-80 %, followed by drying at 60 $^{\circ}$ C in an air oven. The hybrid films are referred as Px(ySA), where 'P' stands for polystyrene, 'SA' stands for amphiphilic-modified alumina particles, 'x' and 'y' represents the percentage loading of SA particles and the Hb/Hp ratio of the particles respectively. SA particles synthesised using AS:VS molar ratio of 1:1, 3:1 and 1:3 are termed as SA11, SA31 and SA13 respectively.

3.3.3. Assessment of amino functionality of BF cavities

3.3.3.1. Ninhydrin Treatment

10mM ninhydrin solution was prepared by dissolving requisite amount of ninhydrin in methanol/water mixture (3v/1v). The patterned hybrid film is then immersed in the solution in a petri dish for 2h under vacuum in order to penetrate the ninhydrin solution into the pores. The film was then taken out and dried to 50°C in an air oven for 1h.

3.3.3.2. Fluorescamine Treatment

Fluorescamine is a spiro compound that is not fluorescent itself but reacts with primary amines to form highly fluorescent products. The fluorescence labelling was carried out with 4 mM fluorescamine solution in methanol/water mixture (3 v/v). The patterned hybrid films were immersed in the solution for 2 h under vacuum. The treated films were taken out, wiped and dried to 50 °C in an air oven for 1h. It was then washed with methanol/water mix.

3.4. RESULTS AND DISCUSSION

It is experimentally observed that PSA suspensions were stable for more than 30 minutes and appeared as a cloudy solution suggesting the presence of particle agglomerates in solution. The agglomerate size of SA particles in polystyrene matrix was measured by Dynamic light scattering (DLS) analysis and discussed in chapter 2. The particle dispersion loading maximum in polystyrene matrix was about 3 wt % as was established by the XRD analysis and surface analysis of ninhydrin treated plain films. The drop cast residue on the glass substrate were difficult to be separated from the substrate without damaging the film. Therefore, the morphological analysis of the films was carried out using the film supported on the substrate.

The drop cast residue of polymer solutions in solvents like THF generally exhibits concentration dependent morphological transition. Therefore, the drop cast residues prepared from PSA/THF suspensions of varying concentration (2.5 to 50 mg/mL) were initially observed under optical microscope to optimize the concentration for forming BF patterned film. The optical images (Figure 3.2) showed that continuous film with relatively uniform microstructure was formed at a concentration of 15 mg/mL. Therefore, the drop cast residues were analysed under SEM for the detailed analysis.

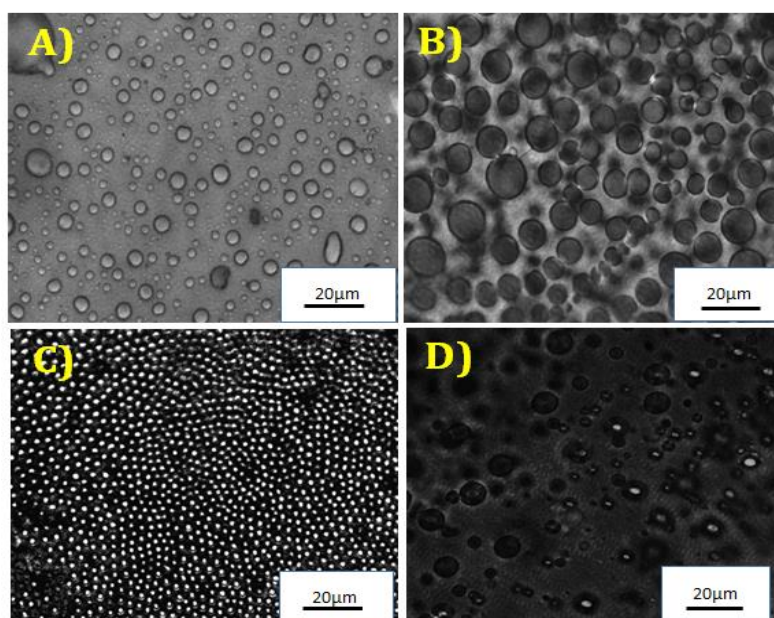


Figure 3.2. Optical microscopic images of drop cast residue of P3(2SA)/THF solution at concentration (a) 2.5 mg/mL, (b) 10 mg/mL, (c) 15 mg/mL, and (d) 25 mg/mL.

Figure 3.3 shows the SEM images of drop cast residue of PSA/THF solution at different concentrations. Whereas the residue from solution concentration of 2.5 mg/mL appeared as disc like aggregates, a film morphology with surface features were observed for the residues from concentration between 10-25 mg/mL and finally a feature less film at a concentration of 50 mg/mL. The patterns appeared to be more uniform at the solution concentration of 15 mg/mL. The above observation

suggested that a concentration of 15 mg/mL is optimum or critical to form BF patterned film from PSA suspensions. The irregular patterns at lower and higher concentrations were attributed to the effect of viscosity of the suspensions. At low concentration, suspension having low viscosity failed to withstand the condensed water droplets with the precipitated layer of polymer bag, while solution of higher concentration having higher viscosity resisted the sinking of the water droplets (Muñoz-Bonilla *et al.*, 2014). The pore size generally depends on various factors like solution concentration, solvent, humidity, etc. However, BFs were not formed in an atmosphere of lower relative humidity of 30-40 %. This was proven by casting and drying the PSA suspensions in a non-humid condition in a glove box and observed feature less film.

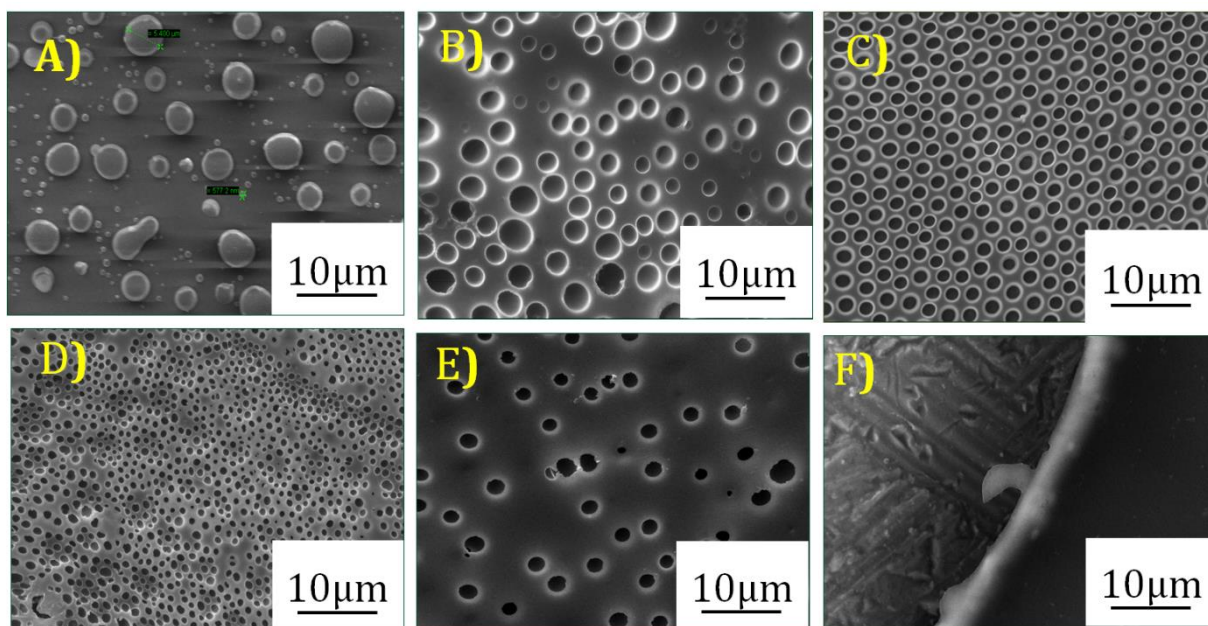


Figure 3.3. SEM images of PSA drop cast from THF solution of concentration (a) 2.5 mg/mL (b) 10 mg/mL (c) 15 mg/mL (d) 20 mg/mL (e) 25 mg/mL and (f) 50 mg/mL.

Figure 3.4 shows the SEM images of the film from 15 mg/mL suspensions at higher magnification along with the cross-sectional image. The patterns exhibited

nearly hexagonally close-packed arrays of concavities having diameter of 1.66 ± 0.08 μm , strut thickness of 1.1 ± 0.22 μm and feature density of 14×10^7 features/ cm^2 (measured by imagej software). The cross-section image (figure 3.5 (C)) indicated a two dimensional array of BF cavities which implies a monolayer formation under the present conditions. On the other hand, the polystyrene film produced by drop casting 15 mg/mL of polystyrene solution in THF (figure 2.5 (D)) failed to achieve any BF features under the same experimental conditions in accordance with the previous results (Ferrari et al., 2011).

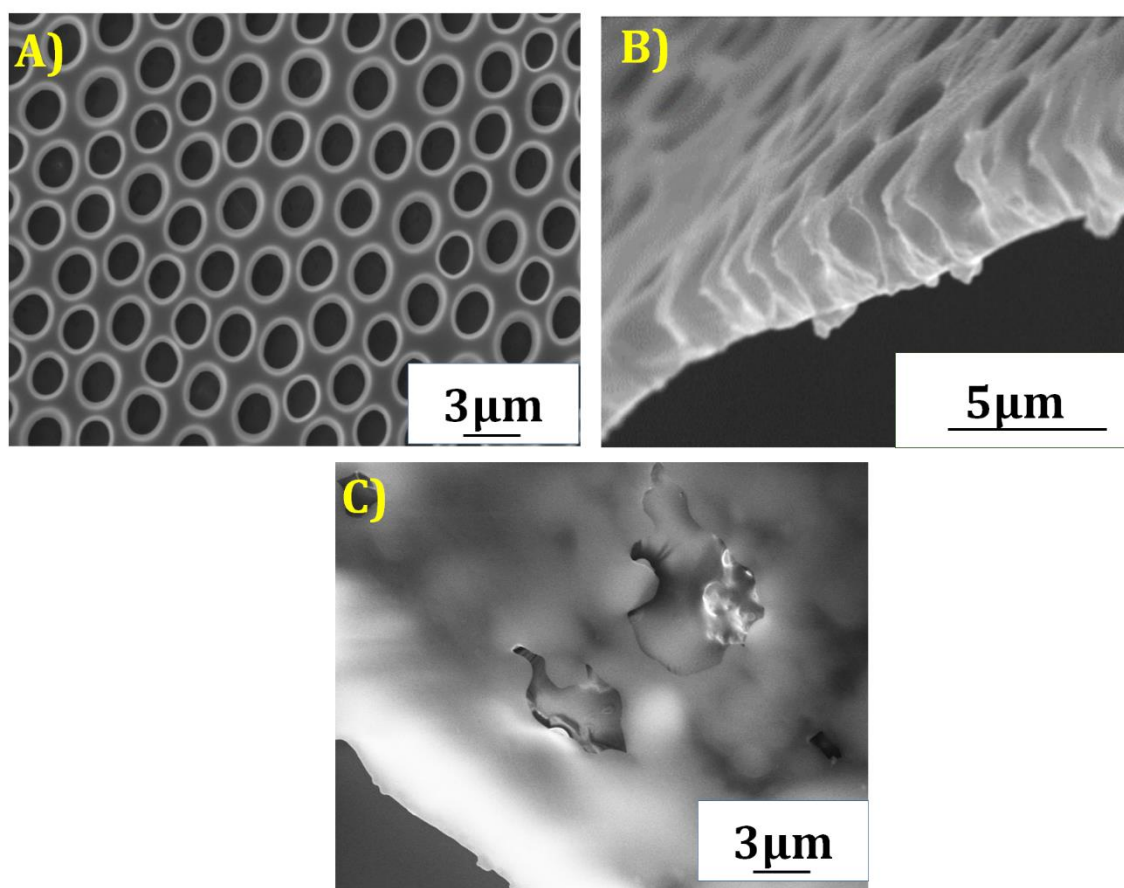


Figure 3.4. SEM images of drop cast residue from PSA suspensions of concentration 15 mg/mL (A) at higher magnification (B) cross-sectional, and (C) SEM image of drop cast residue of neat PS under identical experimental condition.

The BF formation on the PSA hybrid films was again proven by the atomic force microscopic (AFM) images as shown in figure 3.5. The height profile created from the AFM image confirmed the pore size of $1.6 \mu\text{m}$ as was also measured from the SEM images.

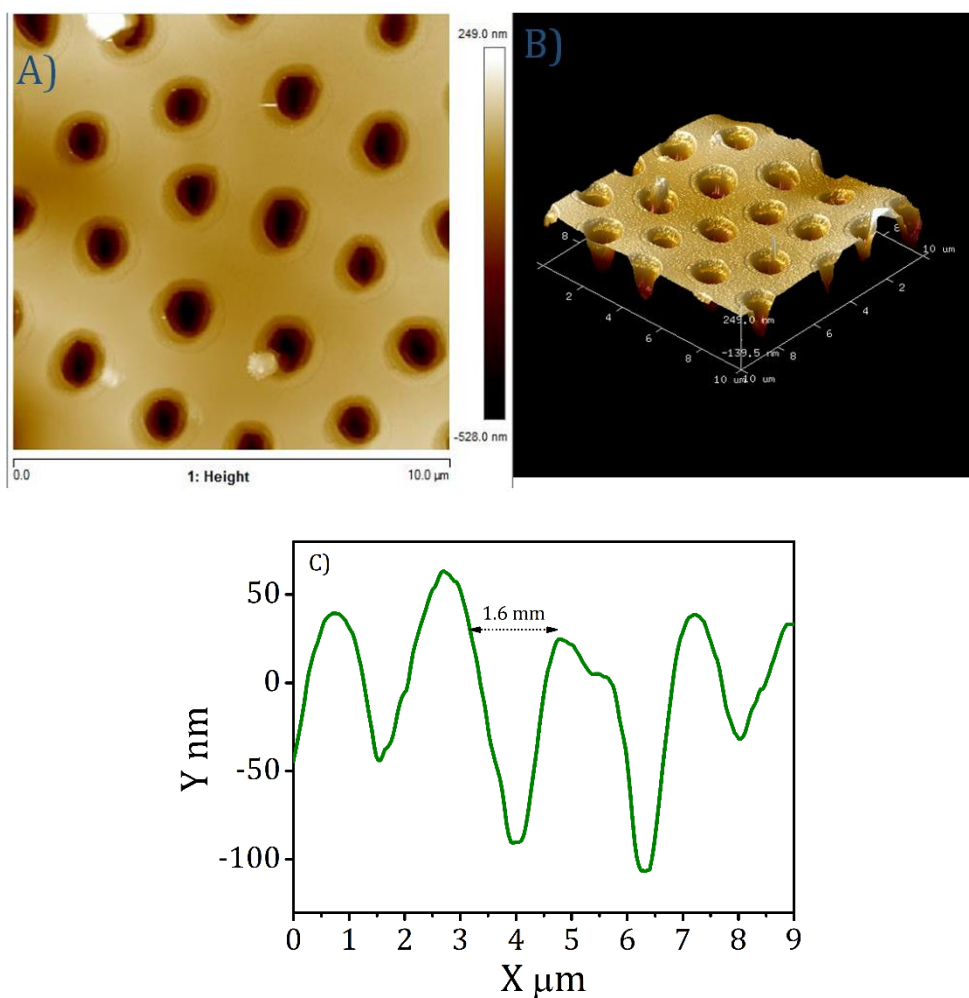


Figure 3.5. (A) AFM image of the drop cast residue of PSA/THF solution. (B) The 3D AFM image of patterned film along with the (C) height profile

3.4.1. BF Mechanism in PSA hybrid film

As mentioned earlier, presence of amphiphilic-alumina particles in the PS/THF suspension aided the formation of breath figures on the hybrid film. This observation suggested a particle-assisted BF mechanism. So far, several discussions

on particle assisted BF mechanism have been reported (*Boker et al., 2004; Sun et al., 2008; Vohra et al., 2009; Sun et al., 2010*). The ability of nanoparticles to assemble at water-droplet/suspension interface by hydrodynamic drag force is well established. The breath figure formation in polymer/nanoparticle hybrid film is a procedure of the combination of breath figure process and so-called "Pickering emulsion" (*Escalé et al., 2012*). A Pickering emulsion is an emulsion that is stabilized by solid particles which adsorb onto the interface between the two phases. The breath figure interface is a clear boundary between the water droplets and the polymer solution. The inorganic particles are dragged towards the interface and these adsorbed particles could stabilize the breath figures formed on the hybrid film. The adsorption energy (E) of the particles at the interface depends on the particle size and the contact angle of the particles at this interface (*Pieranski, 1980*). The value of ' E ' can be larger than the thermal energy $k_B T$ and therefore, the particles will be held to the interface more strongly than surfactant molecules.

Based on the general mechanism mentioned above, the breath figure stabilization in PSA drop cast solution can be described as follows. Fast evaporation of the solvent from PSA suspension followed a reduction in volume/thickness of the film at a rate higher than that of the particle settling rate. As a result, SA particles appeared at the solution surface on which the water droplets preferred to grow even at the early stages of drying. Simultaneously, the amphiphilic alumina particles those resides nearby the droplet as well as in the interior of the solution were dragged towards the droplet/polymer solution interface by Pickering emulsion (*Boker et al., 2004*). Stabilization of the water droplets occurred due to the adsorbed layer of particles at the interface which acted as a mechanical barrier for droplet coalescence.

as a barrier for further dissolution, and stabilize the droplets. Consequently, a particle-assisted breath figure mechanism can be confirmed for the BF formation in PSA hybrid film and demonstrated as shown in figure 3.7.

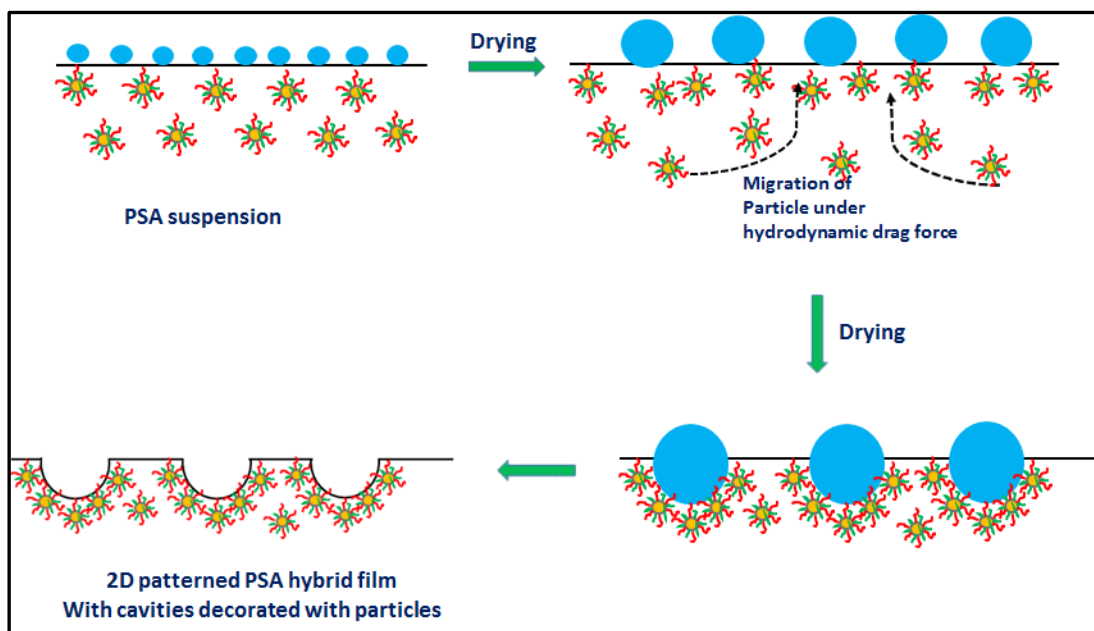


Figure 3.7. Schematic representation of stabilization of breath figures by amphiphilic-modified alumina particles

It should be noted that no particles were seen at the edge of the BF cavity, as they are preferably located at the interior of the cavity wall. Since the particles employed for BF stabilization mechanism were amphiphilic-modified, they were partially immersed in the organic phase. Moreover, the high interfacial tension between the polymer and the water droplet forced the polymer precipitation around the droplet which created a roof over every pore, which masked the underneath particles.

The advantage of amphiphilic nature of the alumina particles lies on their ability to be adsorbed at the BF interface in such a way that the hydrophilic amino group resides at the water phase while polymer chain dispersed in the solvent phase.

Therefore, these amphiphilic-alumina particles can be regarded as a ‘particle-surfactant’ and the adsorption energy of these particles is higher than the easily desorbed surfactant molecules. Moreover, the bi-functionality on the particle surface accomplishes their role in the BF mechanism. The PS chain on the SA particles extend into the PSA suspension and improves the dispersion of the particles whereas the hydrophilic amino group promotes the water condensation and stabilization of BFs on the PSA solution by aligning towards the water droplet.

The alumina particles failed to produce any BF patterns when modified with vinyl silane alone (figure 3.8) which confirms the importance of amino group to attain a stable and uniform breath figures in PSA hybrid film. An added advantage of the amino functionalised amphiphilic alumina nanoparticles is the achievement of amino functionalized BF cavities due to the exposure of amino groups of the particles towards the water phase.

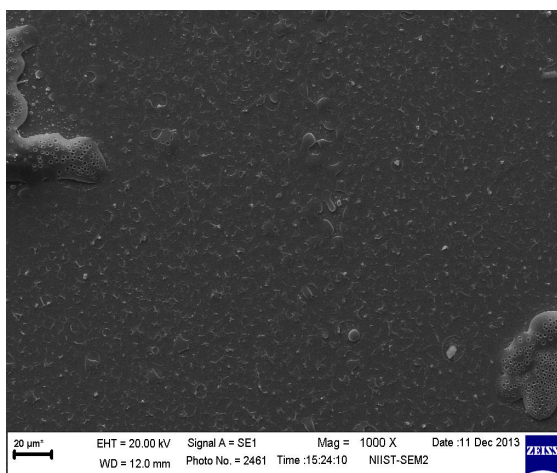


Figure 3.8. SEM image of hybrid film prepared by drop casting PSA solution of alumina particles which were modified with the vinyl silane (VS) alone

The particle agglomeration at the BF interface was confirmed by analysing the XRD spectrum of the patterned film. The XRD plot of patterned film depicted in figure

3.9 in comparison with the plain film showed the reappearance of characteristics peak of alumina ($2\theta = \sim 25.2^\circ$ and $\sim 35.2^\circ$), which confirmed the aggregation of particles due to its migration towards the BF interface.

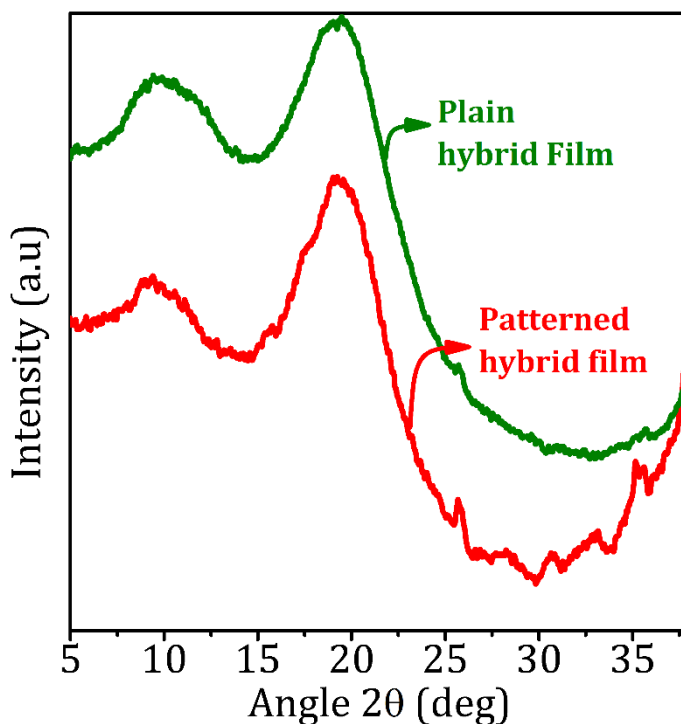


Figure 3.9. XRD pattern of patterned hybrid film in comparison with the plain film

The BF cavity functionalized with amino groups was assessed by treating the patterned hybrid films with ninhydrin (*Kaiser et al., 1970*). We already established the ability of ninhydrin to qualitatively detect the free amino group and the reaction mechanism is as described in chart 2.1. The ninhydrin treated films were analysed under optical microscopy (reflection mode) in comparison with the untreated film (Figure 3.10). The ninhydrin treated patterned hybrid film exhibited dark fringes around the cavity wall and dark colouration inside the cavity in comparison with the non-treated film.

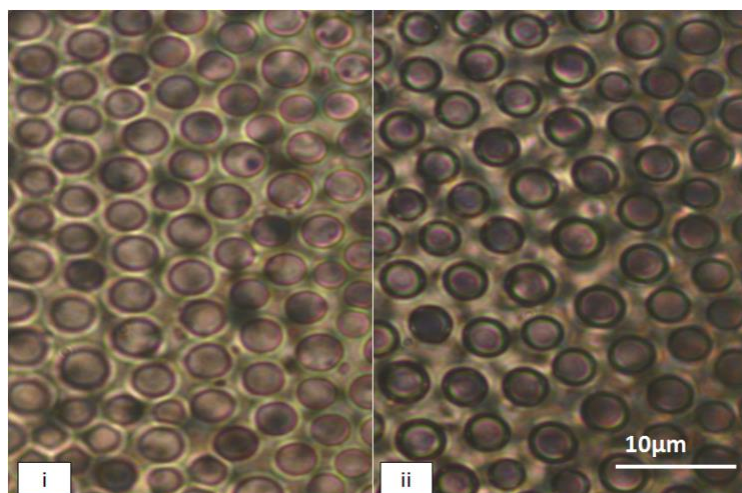


Figure 3.10. Optical microscopy image of patterned hybrid film (i) before and (ii) after treatment with ninhydrin

The occurrence of amino functionalized cavities was further confirmed by the fluorescence microscopic (*Leica Fluorescence Microscope*) images (Figure 3.11) of patterned hybrid film after the treatment with fluorescamine (*Galeotti et al., 2010*). Fluorescamine is a non-fluorescent dye, but forms fluorescent adduct on reaction with free amino group as illustrated in chart 3.1. The fluorescence of the amino-dye complex has an emission wavelength of approximately 470 nm. The fluorescence response is localized at the cavity wall which assured the functionalization of the BF cavities by the amino groups of the particles. The amino rich BF cavities can be demonstrated as shown in figure 3.11 (b).

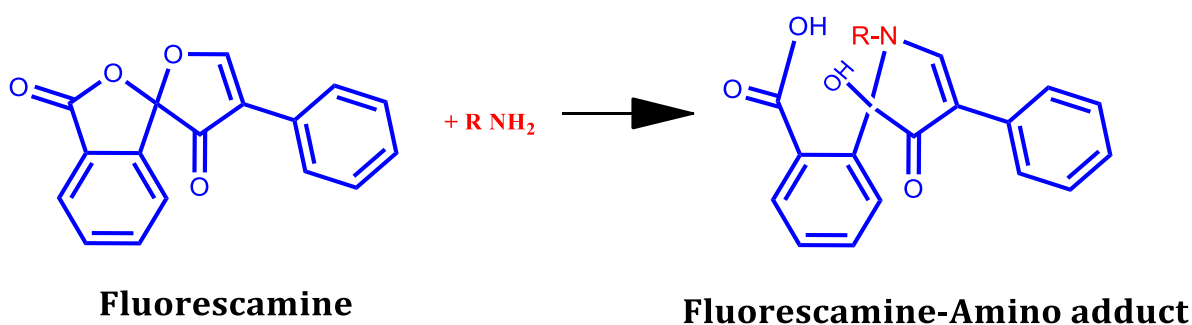
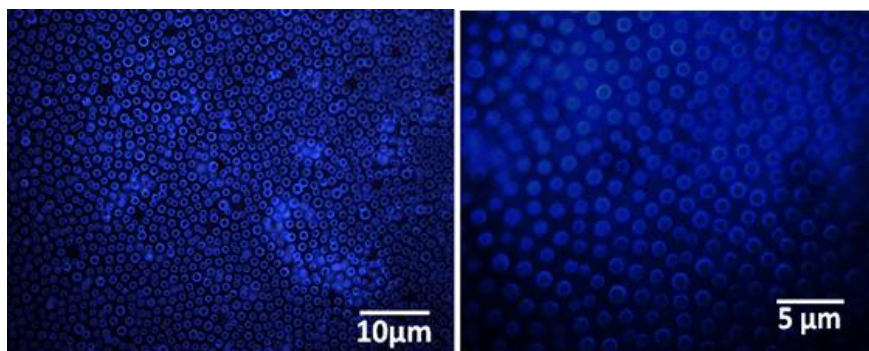
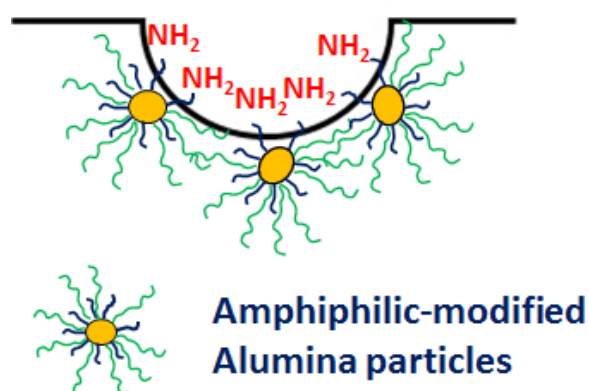


Chart 3.1. Reaction mechanism of fluorescence labelling of patterned hybrid film by fluorescamine



(a)



(b)

Figure 3.11. (a) Fluorescence Spectroscopic image (different magnifications) of patterned hybrid film after treatment with fluorescamine (b) Schematic representation of amino functionalized BF cavity

3.4.2. Effect of particle loading on BF morphology

In a particle assisted BF mechanism, the influence of particle characteristics on the BF morphology cannot be ignored. The influence of particle quantity on the breath figure pattern on hybrid film is of great research interest as they can effectively tune the pore morphology of BFs. It is well known that the physical and chemical properties of the particles could influence the stabilization mechanism of breath figure pattern. We investigated the influence of SA particle concentration on the breath figure morphology by increasing the particle loading from 2-5 wt % (with

respect to polystyrene) in the PSA/THF solution. The 2SA particles were selected for the preparation of PSA suspensions. The SEM images of different hybrid films P2(2SA), P3(2SA), P3.5(2SA), P4(2SA) and P5(2SA) shown in figure 3.12 clearly demonstrated the morphology variation with particle loadings. P2(2SA) showed an irregular arrays of concavities while the microstructure became relatively uniform in P3(2SA) with concavities having diameter close to that observed for P2(2SA) film. When the particle loading increased to 3.5 wt % (P3.5(2SA)), almost same cavity size was observed while the uniformity of the pattern is slightly altered. Further increase in the particle concentration (P4(2SA)) resulted in non-uniform microstructure with concavities having a wide range of diameter (figure 3.12(C)) and finally into a collapsed patterns in P5(2SA). So we can say that pattern become non-uniform on exceeding the particle concentration beyond 3.5 wt%. More specifically, the morphology of the patterns in the composite film was dependent on the particle concentration such that particle concentration of 3-3.5 wt% was critical to form the most closely packed arrays of concavities with diameter in a narrow range. P2(2SA), P3(2SA) and P3.5(2SA) exhibited almost similar BF cavity size of $\sim 1.8 \mu\text{m}$. But the feature density is remarkably high for P3(2SA) film ($14.0 \times 10^7 \text{ cm}^{-2}$) compared to others.

The uniformity or the ordering of the BF patterns was quantitatively evaluated by Voronoi polygons construction. Voronoi polygons are the “smallest convex polygons surrounding points whose sides are perpendicular bisectors of lines connecting a given point with those of its neighbour holes” (*Ferrari et al., 2011*). The regularity of the BF patterns was estimated in terms of the coordination number ‘n’

and P_n (fraction of the polygon having a particular co-ordination number) of the polygon.

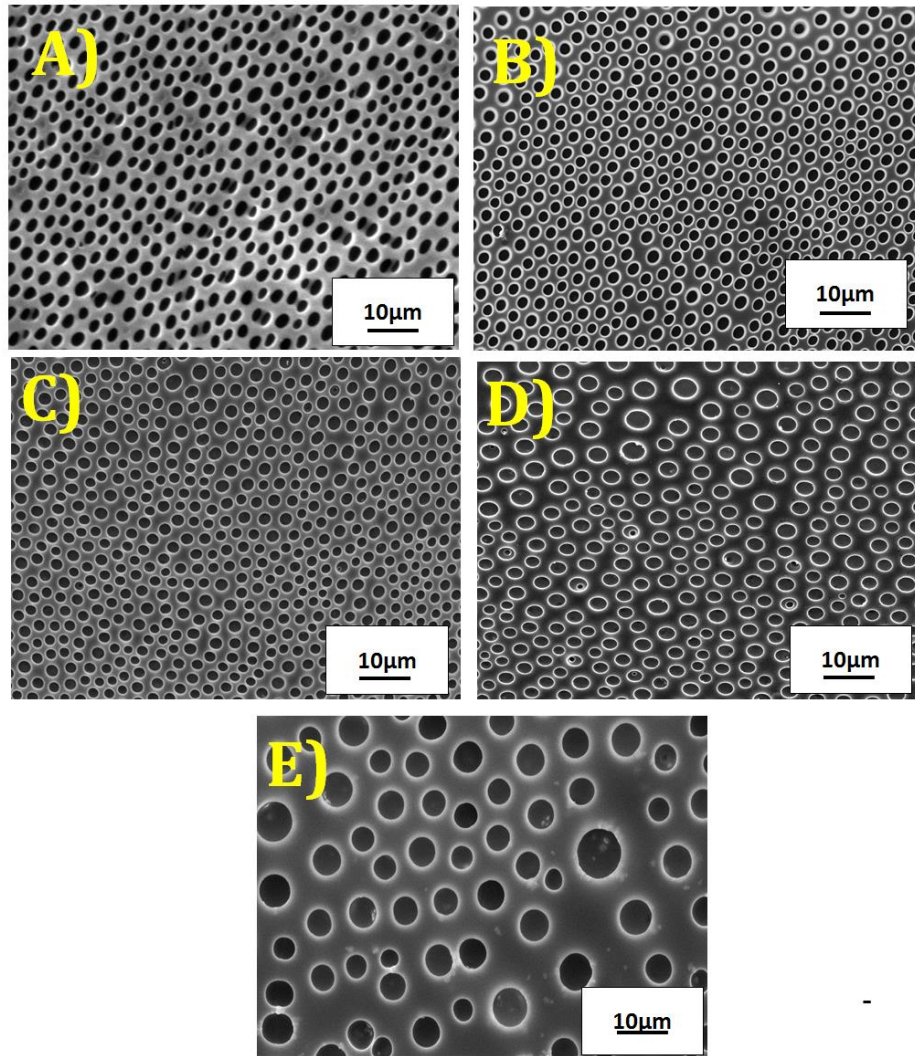


Figure 3.12. SEM images of patterned composite films (a) P2(2SA), (b) P3(2SA), (c) P3.5(2SA), (d) P4(2SA) and (e) P5(2SA) film from THF, showing the effect of particle concentration on pore morphology of BF pattern.

The conformational entropy of the patterns can be calculated by the following equation (Steyer *et al.*, 1990).

$$S = - \sum P_n \ln P_n \text{ ----- (3.2)}$$

For highly random distribution of BF patterns S has a value of 1.71 and zero for a perfectly ordered pattern. In our calculation, we considered 'n' values 4, 5, 6 and

7. The Voronoi polygon constructed for the BF patterns observed on P3(2SA) was presented in figure 3.13 for a general understanding. The lowest S value indicated the maximum ordering of BF patterns. On comparing the S values obtained for P3(2SA) and P3.5(2SA), lower value of S was observed for the former ($S=0.77$) compared to the latter (0.87). Therefore, we could say that as when the particle loading increased from 3 wt % the uniformity of the patterns tends to be reduced. The pore morphology of each hybrid films, in the sense, the pore size, strut thickness, feature density (per cm^2) and conformational entropy measured using imagej with different particle loading is summarized in Table 3.1.

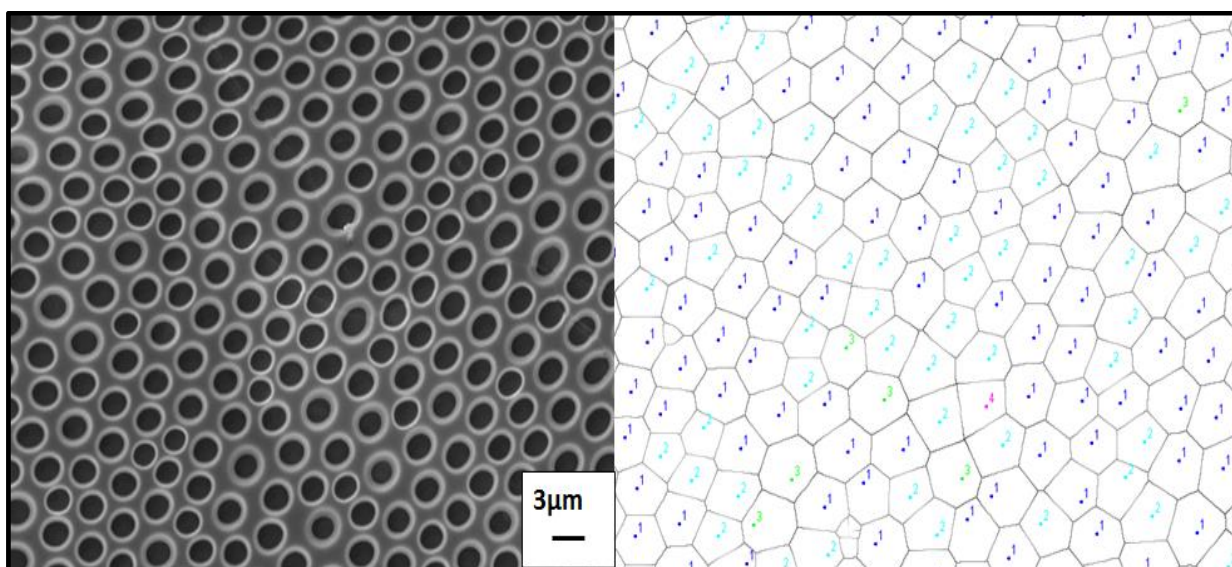


Figure 3.13. Construction of Voronoi Polygon for the BF patterns observed on P3(2SA) hybrid film

From the general understanding of particle-assisted breath figure mechanism, we could say that the capability of water droplet stabilization by the particles increased with the number of particles adsorbed at the interface, at least until a maximum loading limit. It is possible that the fine dispersion of the particles in the PSA suspension upsurge the surface coverage density of the particles thereby

stabilizing the water droplets formed on the solution surface to a great extent. Whereas large agglomerates settled down easily and were not easily carried with the droplets during its transportation to the three phase contact line under hydrodynamic drag force.

Table 3.1. Pore morphological features of different patterned PSA film with varying particle loading

Samples	Pore Size (μm)	Strut Thickness (μm)	Features Density (Cavity/ cm^2)	Conformational Entropy (S)
P2(2SA)	1.87 \pm 0.2	1.6-4.2	3 x10 ⁷	-
P3(2SA)	1.66 \pm 0.11	1.1 \pm 0.22	14.0x10 ⁷	0.77
P3.5(2SA)	1.80 \pm 0.21	1.3 \pm 0.50	9.8 x10 ⁷	0.87
P4(2SA)	2.80 \pm 0.36	0.660-3.1	0.455 x10 ⁷	-
P5(2SA)	1.60-4.2	1.4-4.2	0.196 x10 ⁷	-

In the case of P2(2SA), the number of particles in the suspension was insufficient to stabilize the water droplets in a uniform manner to form regular hexagonal arrays. Practically, this was possible only by dispersing maximum amount of particles in the suspension, as for P3(2SA). Any deviation from this resulted in a non-uniform pattern. The ninhydrin treatment on plain films described in section 2.4.4 established that uniform distribution of particles in the PS matrix occurred at 3 wt % concentration and was regarded as the maximum dispersion loading limit of SA particles in PS matrix. Above the dispersion loading limit, particle agglomeration reduced the effective number of particle domains in the suspension. Apart from that, the inability of the large agglomerates to migrate along with the water droplets during its levitation in the solution for attaining a stable hexagonal structure cannot

limit the later stage coalescence of the droplets. This leads to irregular patterns with varying cavity size in P4(2SA) and P5(2SA).

3.4.3. Effect of Hb/Hp ratio of the particles on BF morphology

The influence of the hydrophobic/hydrophilic (Hb/Hp) balance of the modifiers of the SA particles on the pore morphology of BF patterns from THF was also investigated by fixing the optimized particle loading of 3 wt %. Figure 3.14 shows the SEM images of the BF patterns formed on P3(2SA), P3(2.6SA) and P3(4SA) hybrid films.

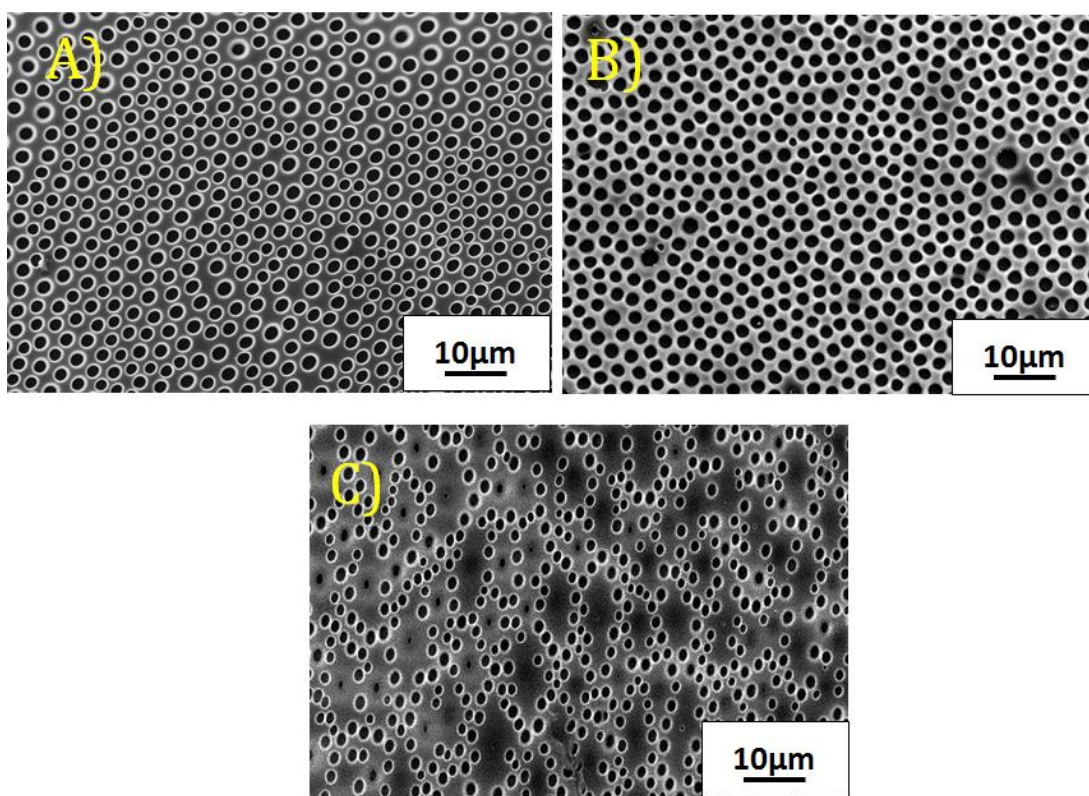


Figure 3.14. SEM images of micropatterned composite films (a) P3(2SA), (b) P3(2.6SA) and (c) P3(4SA) from THF, showing the effect of hydrophobicity of alumina particles on BF pore morphology.

We can see that 2.6SA particles helped to achieve better BF pattern than 2SA and 4SA particles, although the average pore diameter measured from the patterns

was in a close range of 1.56-1.66 μm . On the other hand, the feature density increased from $14 \times 10^7/\text{cm}^2$ for P3(2SA) to $15 \times 10^7/\text{cm}^2$ for P3(2.6A), while P3(4SA) exhibited scattered morphology with very low feature density of $6 \times 10^7/\text{cm}^2$. The conformational entropy (S) calculated for BF patterns on P3(2SA) and P3(2.6SA) film were 0.77 and 0.68 respectively which clearly indicated the improved regularity of the patterns with 2.6SA particles. The pore size, feature density and the conformational entropy of the BF patterns of different hybrid films P3(2SA), P3(2.6SA) and P3(4SA) were summarized in Table 3.2.

Table 3.2. BF cavity size, feature density and conformational entropy of PSA films with varying Hb/Hp ratio

Composite	Cavity size (μm)	Feature density (Cavity/ cm^2)	Conformational Entropy(S)
P3(2SA)	1.66 \pm 0.08	14×10^7	0.77
P3(2.6SA)	1.61 \pm 0.09	15×10^7	0.68
P3(4SA)	1.56 \pm 0.26	6.1×10^7	-

To be specific, the hydrophobic/hydrophilic balance of the particles played a significant role in determining the morphology of BF patterns. In order to explain the observed morphological variation, dispersion and suspension stability of the particles in PS/THF solution at the varying hydrophobicity of the particle has to be considered. Obviously, increased hydrophobicity improved the dispersion of the particles in PS/THF solution thereby enhancing the number advantage of particles towards the water droplet-solvent interface. So the regularity and pore density increased with the increase in the dispersion of the particles. The DLS analysis of the

SA particle agglomerates in PS/THF suspension were discussed in chapter 2. We observed an improvement in dispersion with the Hb/Hp ratio of the particles. The water miscible THF solvates the amino moiety and an electro-steric stabilization is likely to happen in these circumstances which promoted the dispersion of even 2SA particles. The particle dispersion in PS solution was further enhanced by the increase in the PS chain length on the 2.6SA particles. This resulted in the elevation of fine particle domain on the solution surface thereby increasing the regularity and feature density in its hybrid film.

Nevertheless, we were observing a defective pattern for P3(4SA) in contrast to an increase in the uniformity. As the hydrophobicity of the 4SA particles is increased, although an effective dispersion was expected, the stabilization capability of particles at the BF interface was reduced. This might be due to the fact that, enhanced interaction between 4SA particles and the THF solvent was expected due to the increased chain length. So the highly hydrophobic 4SA particles reside more on the solvent phase in the diffusion layer of THF and condensed water droplet. The solvated amino group cannot drag the particles effectively into the water phase resulting in diffusion layer enlargement which led to an irregular pattern. Figure 3.15 represents the stabilization mechanism operating at the THF/water interface of PSA drop cast solution with 2SA, 2.6SA, and 4SA particles. This made us conclude that there should be a balance between the hydrophilic to hydrophobic ratio for the particles to stabilize the water droplets effectively in the polar solvent like THF.

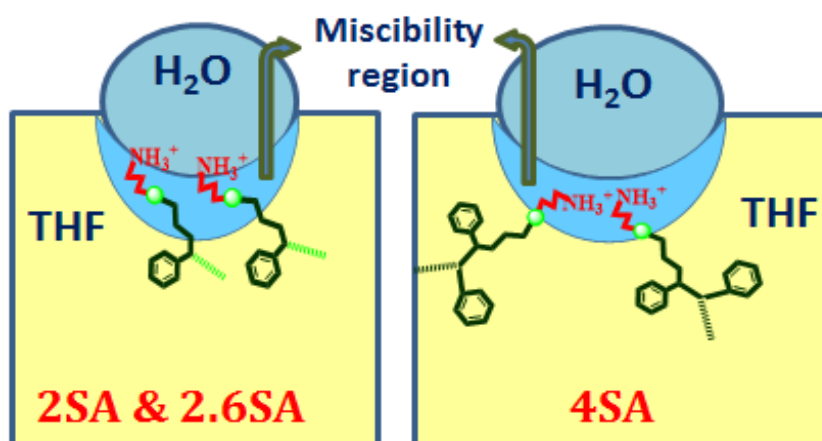


Figure 3.15. Schematics representation of stabilization mechanism of BF cavity interface of THF and water by 2SA, 2.6SA and 4SA particles

3.4.4. Breath Figure Formation with SA31 and SA13 particles

The SA31 and SA13 particles were dispersed in tetrahydrofuran and the stability of the suspensions were observed visually. It was found that SA31 particles with styrene/alumina molar ratio greater than 0.09 were stable in suspension for more than 30 min whereas SA13 particles showed good dispersion even without polystyrene modification, but the modification with S/A ratio minimum of 0.03 was necessary for the suspension stability. Hb/Hp values of the particles were calculated from their TGA data as described in chapter 2. Figure 3.16 shows the TG curves for SA31 and SA13 particles. The amount of the hydrophilic amino group and hydrophobic polystyrene and the resulting Hb/Hp balance are summarised in Table 3.3. The SA particles are referred as xSA31 and xSA13, where x is the S/A ratio.

SA31 and SA13 particles having Hb/Hp value of 2.2 and 2.9 respectively were used for preparing the patterned films. Figure 3.17 shows the SEM images of the patterned films from THF.

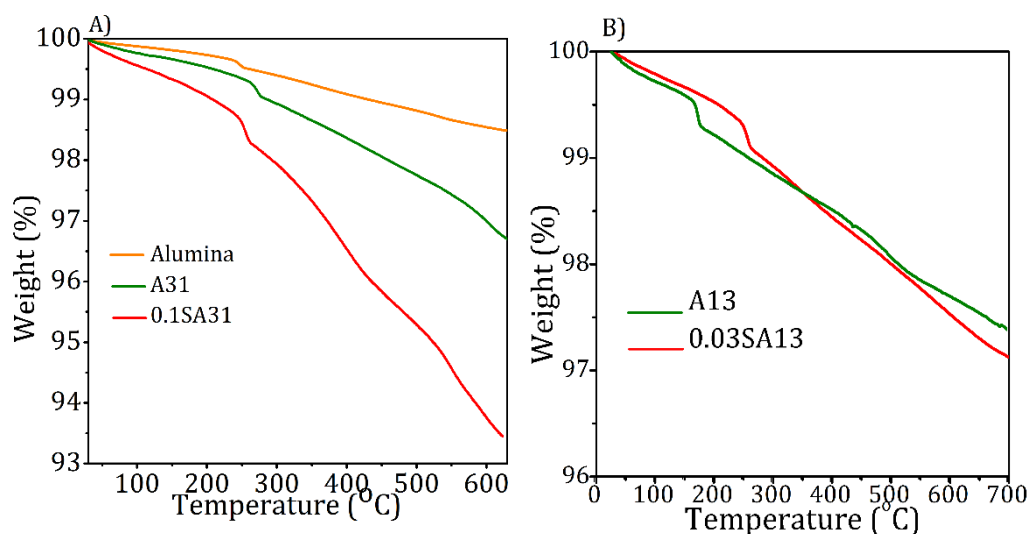


Figure 3.16. TG curve of (a) 0.1SA31 and (b) 0.03SA13 particles.

Table 3.3. Calculation of Hb/Hp ratio of 0.1SA31 and 0.03SA13 particles

Samples	Total Weight Loss (%)	Weight Loss due to silane (%)			Loss due to PS (%)	Hydrophilic (Hp) %	Hydrophobic (Hb) %	Hb/Hp ratio
		Total	AS	VS				
A	1.1	-	-	-	-	-	-	-
A31	3.2	2.1	1.63	0.46	-	-	-	-
0.1SA31	6.5	2.1	1.63	0.46	3.2	1.7	3.68	2.2
A13	2.59	1.49	0.43	1.06	-	0.43	1.06	2.5
0.03SA13	2.8	1.49	0.43	1.06	0.2	0.43	1.26	2.9

It is evident from the figures that P3(2.2SA31) film formed relatively uniform BF pattern while P3(2.9SA13) failed to achieve a regular pattern. The average pore size, feature density and conformational entropy for P3(2.2SA31), measured from the SEM images using imagej, were $2.5 \pm 0.14 \mu\text{m}$, $7.5 \times 10^7/\text{cm}^2$ and 1.09 respectively. These morphological features for P3(2.9SA13) significantly deviated from above

values such that the average pore size and feature density measured were 1.2 ± 0.33 μm and $2.3 \times 10^7 / \text{cm}^2$ respectively

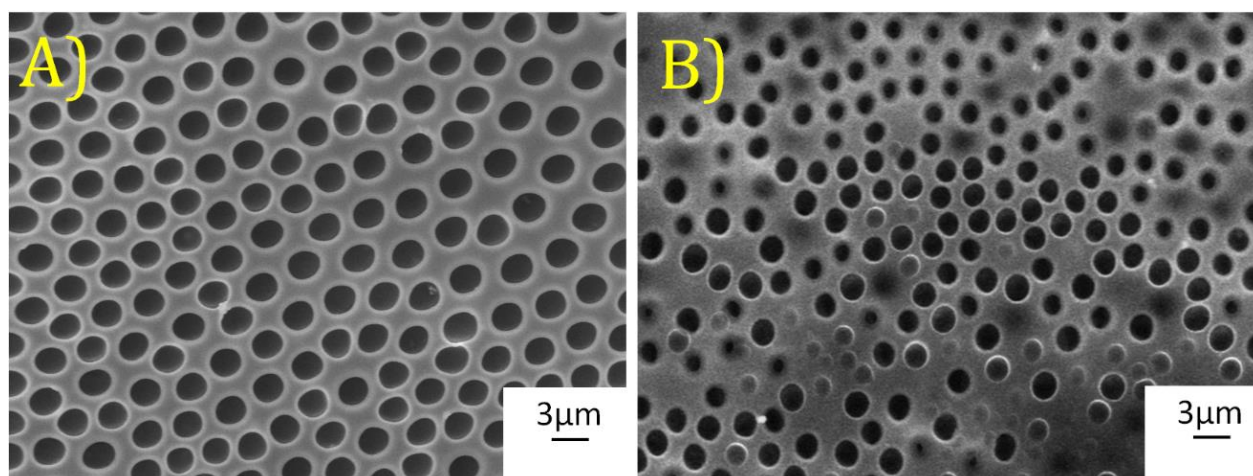


Figure 3.17. SEM images of the drop-cast residue of (a) P3(2.2SA31) and (b) P3(2.9SA13)

Table 3.4. Breath figure cavity size, feature density and conformational entropy of P3(2.6SA11), P3(2.2SA31) and P3(2.9SA13) hybrid films

Composite	BF Cavity size (μm)	Feature density (Cavity/ cm^2)	Conformational Entropy(S)
P3(2.6SA11)	1.61 ± 0.09	15×10^7	0.68
P3(2.2SA31)	2.5 ± 0.14	7.5×10^7	1.09
P3(2.9SA13)	1.2 ± 0.33	2.3×10^7	-

The morphological features of the films using SA11, SA31 and SA13 particles are summarised in Table 3.4 for comparison. It can be seen that the most uniform pattern was obtained for P3(2.6SA11) followed by P3(2.2SA31). It may be noted that P3(2SA11), P3(2.6SA11) and P3(4SA11) films from THF exhibited pore size values of $1.89 \mu\text{m}$, $1.61 \mu\text{m}$ and $1.56 \mu\text{m}$ respectively (see chapter 3). Here, 2SA, 2.6SA and 4SA

particles showed almost identical dispersion characteristics and individual SA11 particles are expected to carry amino groups of identical concentration. Yet the cavity size increased as the hydrophilicity increased. It appeared that the interfacial layer of the particles at the water/THF interface stretch the droplets outward under the attractive force from THF. Assuming that each droplet carries equal number of particles at the interface, the extent of stretching is likely to depend on the concentration of the amino groups. This would explain the above observed increase in the cavity size with increase in the hydrophilicity or Hb/Hp value of the SA11 particles. Under identical conditions, the droplet would carry equal number of SA31 particles at the interface, but carrying 3 times of the hydrophilic amino groups. Consequently, the droplets carrying the SA31 particles would experience higher stretching force than of SA11 particles and lead to higher cavity. Accordingly, P3(2.9SA13) should show low cavity size, as the experimentally observed.

3.5. CONCLUSION

In summary, we have fabricated amino-functionalised breath figure patterns on polystyrene alumina (PSA) hybrid film using glass substrate by simple drop casting technique. The amino functionalization inside BF cavity was achieved by amino functionalized amphiphilic-alumina (SA) nanoparticles, and these particles were found to be a suitable candidate for stabilizing the BFs formed on the hybrid film surface even with water miscible solvent like THF. Moreover, the physical and chemical properties of the alumina particles such as particle concentration and hydrophobicity could influence the BF morphology. The study revealed that uniform breath figure pattern was achieved at a maximum dispersion loading of the particles, i.e. 3 wt % with respect to polystyrene and any deviation from this altered the

regularity of the pattern. The impact of hydrophobicity of the SA particles on the BF morphology was probed by using SA particles having different Hb/Hp ratios, such as 2SA, 2.6SA, and 4SA particles and found that 2.6SA particles could produce a regular BF patterns with a conformational entropy (S) of 0.68. Therefore, it can be concluded that there should be a balance between the hydrophobic to hydrophilic ratio of the modifier on the nanoparticle surface for the effective stabilization of BFs in the polar solvent like THF. The most uniform BF pattern was observed for P3(2.6SA) hybrid films which exhibits the pore morphological features such as pore size of 1.61 ± 0.09 μm , and feature density of $15 \times 10^7 / \text{cm}^2$. The BF patterns produced using SA31 and SA13 particles could generate comparatively less uniform patterns. The conformational entropy of the most uniform BF patterns produced using SA31 particles, i.e. P3(2.2SA31) is 1.09 while SA13 particles produced highly irregular pattern. The remarkable achievement of our investigation is the amino group embedded BF cavities which find several advanced applications in various industrial and biological fields owing to its active nature and ease of further modification by simple substitution reactions.